JOURNAL OF BACTERIOLOGY, Dec. 1995, p. 6798–6803 Vol. 177, No. 12
0021-9193/95/$04.00+0

Subunit Interactions and Protein Stability in the Cyanobacterial Light-Harvesting Proteins

TRACEY PLANK, COLLEEN TOOLE, AND LAMONT K. ANDERSON*

Department of Biological Science, University of Tulsa, Tulsa, Oklahoma 74104

Received 7 June 1995/Accepted 30 August 1995

Strain 4R is a phycocyanin-minus mutant of the unicellular cyanobacterium *Synechocystis* sp. strain 6803. Although it lacks the light-harvesting protein phycocyanin, 4R has normal levels of phycocyanin (*cpc*) transcripts. Sequence analysis of the *cpcB* gene encoding the phycocyanin β subunit shows an insertion mutation in 4R that causes early termination of translation. Other work has shown that the phycocyanin α subunit and the linker proteins encoded on the *cpc* transcripts are all functional in 4R, yet the defective phycocyanin β subunit results in the complete absence of the α subunit and the linkers. Phycocyanin-minus mutants were constructed in a wild-type background by interruption of *cpcB* and *cpcA* with an antibiotic resistance gene and were compared with the 4R strain. Immunoblot analysis of the mutants demonstrated that interruption of one subunit was accompanied by a complete absence of the unassembled partner subunit. Phycocyanin assembly begins with the formation of the αβ heterodimer (the monomer) and continues through higher-order trimeric and hexameric aggregates that associate with linker proteins to form the phycobilisome rods. The results in this paper indicate that monomer formation is a critical stage in the biliprotein assembly pathway and that unassembled subunits are subject to stringent controls that prevent their appearance in vivo.

Light harvesting in cyanobacteria is mediated by the phycobilisomes, which are complex protein structures located on the surface of the photosynthetic membrane (20). The major structural components of the phycobilisome are the biliproteins, which contain covalently attached bilin chromophores that constitute a resonance energy transfer pathway. Light energy in the 500- to 650-nm range can be absorbed by different classes of biliproteins and is rapidly and efficiently transferred through the phycobilisome to chlorophyll complexes in the photosynthetic membrane. The three major classes of biliproteins are distinguished by their spectral properties. The allophycocyanins (AP [λ_{max} = 650 to 665 nm]) are located in the core of the phycobilisome, which is in direct contact with chlorophyll complexes in the membrane. Phycocyanin (PC [λ_{max} = 617 nm]) is found in the rod substructures that are attached to the phycobilisome cores. A third major biliprotein, phycoerythrin (PE [λ_{max} = 565 nm]), is synthesized in some cyanobacteria and is attached to PC at the periphery of the rod substructures. Each biliprotein has the same subunit organization that is based on a heterodimer (called a monomer by convention) composed of α and β subunits (11, 16, 37–39). Monomers are assembled into disc-like trimers with a central channel, which then stack to form a hexamer in the PC and PE biliproteins. Hexamers are associated with single copies of linker proteins that direct their assembly into the rod substructures. The organization of biliproteins within the phycobilisome structure establishes an energy transfer pathway, PE to PC to AP to chlorophyll, that operates at close to 100% efficiency (7, 19, 20).

Phycobilisomes are not required for phototrophic growth in white light, and assembly mutants have been useful in establishing protein function and phycobilisome architecture (1, 3, 10, 17, 28, 29). The phycobilisome can constitute 30% of the cellular dry mass and represents a major biosynthetic investment for the cyanobacterium. While they are generally not lethal, mutations that disrupt phycobilisome assembly may force a cellular response to the accumulation of unassembled proteins. In some mutants, unassembled material is stable and may remain soluble in the cell (10) or form inclusion bodies (4). Mutations that remove a biliprotein subunit from the assembly process often result in the complete loss of other phycobilisome components (7, 40), suggesting rapid degradation or downregulation of the stranded proteins. An examination of phycobilisome mutants that emphasizes the fate of defective or unassembled proteins may reveal control features that the cell uses to manage the efficient production of these light-harvesting complexes. Some mutants may also provide experimental access to the in vivo pathways that produce a complete phycobilisome.

Strain 4R is a PC-minus mutant of *Synechocystis* sp. strain 6803 that synthesizes intact phycobilisome cores but shows no traces of PC subunits or PC-associated proteins. We have used 4R as a transformation host for the *cpc* genes from *Synechocystis* sp. strain 6701 (2) and have demonstrated the rescue of 4R PC α subunits and PC-associated linker proteins by heterologous assembly (31). The present report establishes that the PC-minus phenotype in *Synechocystis* sp. strain 6803 4R is due to a mutation in the *cpcB* gene that removes the last 80% of CpcB by premature termination of translation. Interposon mutants interrupted in *cpcA* or *cpcB* were constructed for comparison with 4R, and the phenotypes of these strains indicate that stranded biliprotein subunits are not stable when they cannot bind to their assembly partner.

MATERIALS AND METHODS

Bacterial strains and growth conditions. All strains and plasmids used in this study are listed in Table 1. The transformable unicellular cyanobacterium *Synechocystis* sp. strain 6803 and its derivatives were maintained on BG-11 medium (34) supplemented with 1% Bacto-Agar (Difco) and 10 mM *N*-2-hydroxyethylpiperazine-*N*′-2-ethanesulfonic acid (HEPES; pH 8.0). Liquid BG-11 cultures were supplemented with 20 mM glucose–20 mM HEPES (pH 8.0) and were bubbled with 1 to 2% CO_2 in air at room temperature under four warm-white fluorescent lights. The wild-type (WT) and PC-minus (4R) strains of *Synechocystis* sp. strain 6803 were obtained from Dzelkalns and Bogorad (Department of

* Corresponding author. Mailing address: Department of Biological Science, University of Tulsa, 600 S. College Ave., Tulsa, OK 74104. Phone: (918) 631-3328. Electronic mail address: biol_lka@centum.utulsa.edu.

TABLE 1. Bacterial strains and plasmids used in this study

Strain or plasmid	Relevant property(ies)	Reference or source
E. coli		
DH5α	Host strain for plasmid propagation	Gibco BRL
Synechocystis sp. strain 6803		
WT	Wild type strain; *cpcB*$^+$ *cpcA*$^+$	V. Dzelkalns
4R	PC-minus phenotype	V. Dzelkalns
R38	4R complemented to PC-plus phenotype by pPC338	This study
R38KA	4R *cpcA*::*kan* (by pPC38KA)	This study
W38KA	WT *cpcA*::*kan* (by pPC38KA)	This study
W38KB	WT *cpcB*::*kan* (by pPC38KB)	This study
Plasmids		
pBluescriptSK$^-$	Ap^r	Stratagene
pPC338	*cpcB*$^+$ *cpcA*$^+$ (3.8 kbp) in pBluescriptSK$^-$	This study
pPC396	*cpcB*$^+$ *cpcA*$^+$ (9.6 kbp) in pBluescriptSK$^-$	This study
pPC38KA	pPC338 *cpcA*::kan	This study
pPC38KB	pPC338 *cpcB*::kan	This study

Biology, Harvard University). Cyanobacterial transformants (43) were primarily obtained by exposing 20-fold-concentrated mid-log-phase cells to plasmid DNA (5 μg of DNA per ml of cells) for 8 to 10 h in white light. The cells were then diluted 15-fold in BG-11 and grown under standard liquid culture conditions for 72 h. After 10× concentration, 0.1 to 0.3 ml of the cells was placed on BG-11 agar supplemented with 20 mM glucose and 10 μg of kanamycin per ml. Kanamycin-resistant transformants were maintained on selective solid medium through numerous transfers to allow segregation and were tested for genetic homogeneity in the insertion region by Southern hybridization analyses. Conversion of the 4R mutant to the WT phenotype with plasmids pPC396 and pPC338 was accomplished by a top agar method (13). *Escherichia coli* DH5α was used for all plasmid propagation and was grown according to standard protocols (36).

Recombinant methods and DNA and RNA analyses. Unless otherwise stated, DNA manipulations and analyses were performed according to established protocols (36). The *cpc* genes from *Synechocystis* sp. strain 6803 WT were cloned from two different restriction endonuclease-enriched fractions of chromosomal DNA. The presence of *cpc* genes in plasmid libraries and recombinant clones was assessed by PCR (35) with heterologous primers specific to the *cpcBA* operon from *Synechocystis* sp. strain 6701 (2). A 9.6-kbp *Eco*RI-*Pst*I fragment containing *cpcBAHID* was inserted into the commercial vector pBluescriptSK$^-$ (Stratagene), creating pPC396. A 3.8-kbp *Avr*II-*Nhe*I fragment containing *cpcBAH* and part of *cpcI* was inserted into pBluescriptSK$^-$, creating pPC338 (see Table 1 and Fig. 5). The *cpcB* sequence from strain 4R was obtained by cycle sequencing with CircumVENT polymerase (New England Biolabs) with 700-bp double-stranded DNA templates that were amplified from 4R chromosomal DNA with *Taq* polymerase (Perkin-Elmer). The amplification primers were designed to hybridize at sites 60 bp upstream of the *cpcB* translation start codon and 100 bp downstream of the *cpcA* start codon. Interposon mutations in *cpcA* and *cpcB* of *Synechocystis* sp. strain 6803 WT were constructed by insertion of a neomycin phosphotransferase gene at specific restriction sites in the *cpcBAHID* operon as described in the Results section. Cyanobacterial chromosomal DNA was isolated from cyanobacteria by using a large-scale protocol developed from a microscale method (9). Restriction endonuclease digests, agarose gel electrophoresis, and Southern hybridization studies with ^{32}P-labeled probes were performed according to standard protocols (36). mRNA was isolated (33) and was used for Northern (RNA) hybridization analysis according to previously published methods (2) with ^{32}P-labeled genes from *Synechocystis* sp. strain 6803 as probes.

Polyclonal antibodies and immunoblot methods. Purified phycobilisome preparations (4) from *Synechocystis* sp. strain 6803 WT were electrophoresed by high-resolution sodium dodecyl sulfate-polyacrylamide gel electrophoresis (SDS-PAGE). The denatured, isolated PC α and β subunits were obtained by electroelution from gel slices and were combined with a polyA · polyU adjuvant (23) for injection into dwarf New Zealand White rabbits. Serial injections of antigen, serum harvesting, protein transfer from polyacrylamide gels to nitrocellulose, and immunoblot analyses were performed according to standard protocols (22). Clarified serum was used at a 1:250 dilution, and protein-A peroxidase (Boehringer Mannheim) was the secondary binding component in all immunoblots. Antibodies were tested for their abilities to detect CpcA and CpcB in immunoblots of phycobilisome preparations, purified PC, and high-pressure liquid chromatography (HPLC)-purified subunits. Anti-CpcA appears to detect a single band in *Synechocystis* sp. strain 6803 phycobilisomes and also reacts with purified CpcA. Anti-CpcB detects two proteins in phycobilisomes and purified PC, CpcB and a protein that comigrates with CpcA and apo-CpcB. Anti-CpcB does not detect HPLC-purified CpcA. The unidentified protein signal may result from cleavage of CpcB or chromophore loss during preparation procedures.

Cyanobacterial cell extracts. Cell extracts of soluble proteins were obtained from *Synechocystis* sp. strain 6803 strains for SDS-PAGE and immunoblot studies. Mid-log-phase cells (2×10^7 to 3×10^7 cells per ml) were harvested by centrifugation and were resuspended in 50 mM Na-K-PO_4 (pH 7.2)–0.1 mM phenylmethylsulfonyl fluoride (PMSF) at 10 ml/g (fresh weight). The cells were combined with an equal volume of 0.1-mm-diameter zirconium beads and agitated in a Bead Beater (Bio-Spec Products) for three times of 1 min each, with 30-s intervals on ice. Other protease inhibitors were added in some cases as described in the text. After removal of the settled beads, large membrane fragments and unbroken cells were cleared by centrifugation at 13,000 × *g* for 30 min at 4°C. The supernatants were recovered for use as the soluble protein cell extracts and were stored at −20°C. Cell extracts were normalized for AP content by absorbance measurements, and samples of 8 to 12 μg of AP were loaded in each lane for SDS-PAGE.

PAGE. Standard SDS-PAGE was performed in a 10-cm 4 to 20% acrylamide gradient gel according to the method described by Laemmli (27) with modifications to buffer concentrations and acrylamide stocks (4). The fluorescent biliproteins were visualized in the gels prior to Coomassie staining by treatment in 1 mM $ZnSO_4$ (32) and illumination on a UV light transilluminator. High-resolution SDS-PAGE for immunoblot analysis was performed as described above with the following exceptions: a 20-cm 10 to 18% acrylamide gradient gel was used, and the acrylamide stock solution for this gel was 30:0.8 acrylamide-to-bis-acrylamide. SDS-PAGE in the presence of 8 M urea (6) was performed with a 10-cm 15% acrylamide gel made from a 60:0.8 acrylamide-to-bis-acrylamide stock solution.

Synthesis of apo-PC subunits by in vitro transcription-translation. PC subunits without chromophores were generated by in vitro transcription-translation from a plasmid template (pPC02) with an *E. coli* S-30 system (Promega) and T7 RNA polymerase. Plasmid pPC02 is a pBluescriptSK$^-$ derivative that contains a 2.4-kbp fragment of *Synechocystis* sp. strain 6701 DNA encoding the *cpcBA* operon. The reaction mixes included rifampin to prohibit transcription from the *lac* promoter of the plasmid (42).

Other methods. Absorbance spectra of proteins and whole cells were obtained on a Shimadzu UV2101PC spectrophotometer. Whole-cell absorbance spectra were obtained through the opaque sides of the cuvettes to compensate for light scattering by intact cells. Images of culture plates, gels, immunoblots, and autoradiograms were captured with a UVP Imagestore 7500 and were prepared for publication by using Aldus Photostyler 2.0. The X-ray crystal structures of PC from *Agmenellum quadruplicatum* (37, 39) and *Fremyella diplosiphon* (12) were examined with RasMol, a molecular visualization software program written by Roger Sayle (Glaxo Research and Development).

RESULTS

Characterization of *Synechocystis* sp. strain 6803 4R. Colonies of the 4R strain have an olive-green pigmentation that clearly distinguishes them from the blue-green *Synechocystis* sp. strain 6803 WT, suggesting a decreased level of PC. The absorbance spectrum of intact WT cells shows their PC content in the major peak to be near 625 nm, while the 4R cell spectrum is flat in this region (Fig. 1). The absence of PC in 4R was confirmed by SDS-PAGE comparison of phycobilisomes and cell extracts from WT and 4R (Fig. 2). The 4R phycobilisomes are core substructures that lack all rod components, including both PC subunits and the three rod-associated linker proteins (compare lanes 1 and 2), and are similar to the core structures that have been characterized in a mutant of *Synechocystis* sp. strain 6701 (3). The 4R strain does not appear to have any soluble PC, since cell extracts do not show the zinc-enhanced fluorescence signals of PC subunits that are visible in the WT extract (lanes 3 to 6). The membrane pellets from 4R cell extracts were also negative for PC content on the basis of zinc-enhanced fluorescence in SDS-PAGE samples (data not shown).

The apparent absence of PC subunits in 4R is not caused by a lack of *cpc* transcripts. A 700-bp DNA fragment that includes all of *cpcB* and the first 20% of *cpcA* was generated by amplification with *Taq* polymerase with pPC338 as a template. Northern (RNA) hybridization analysis with this probe against 5 μg of WT and 4R mRNA (Fig. 3, lanes 1 and 2) shows the

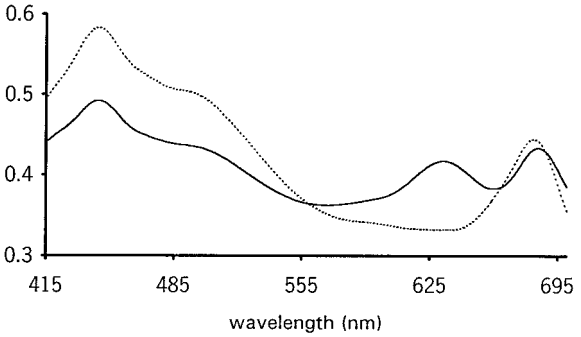

FIG. 1. Absorbance spectra of intact cells from WT and 4R WT cells (——) show a major signal near 625 nm, indicating the presence of PC; 4R cells (– – – – – –) do not synthesize measurable PC in this assay. O.D., optical density.

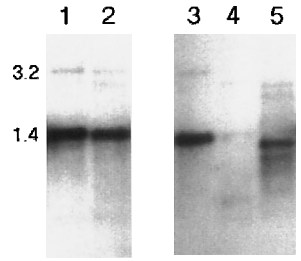

FIG. 3. Northern hybridization analysis of cpcBA transcripts. Each lane contains 4 μg of RNA. Lanes: 1, WT; 2, 4R; 3, R38; 4, W38KB; 5, W38KA. Transcripts encoding *cpcBA* (1.2 kb) and *cpcBAHID* (3.2 kb) are identified by molecular masses shown to the left of lane 1. Gel images were obtained with a UVP Imagestore 7500 and were composed as figures with Aldus Photostyler software on PC-compatible hardware.

presence of 1.4- and 3.2-kb transcripts in both strains. The 1.4-kb mRNA represents the major transcript from *cpcBA* that encodes the PC β and α subunits. The less-prominent 3.2-kb transcript encodes more of the operon, *cpcBAHID*, as was determined with a probe specific for the linker genes *cpcH* and *cpcI* (data not shown). The level of the *cpcBA* transcript in 4R is comparable to that seen in WT, indicating that expression of this operon in 4R is not sufficiently reduced to account for the PC-minus phenotype.

The PC-minus phenotype of *Synechocystis* sp. strain 6803 4R can be complemented by the introduction of the *cpcBA* operon from *Synechocystis* sp. strain 6701 (31). The resulting transformants synthesize phycobilisomes with hybrid rod structures that consist of PC from the introduced *cpcBA6701* genes and linker proteins expressed from the *cpcH* and *cpcI* genes of 4R. Some PC α subunit (CpcA) from the 4R *cpcA* gene is also detected in these phycobilisomes. These observations lead to two conclusions: the *cpc* transcripts that are present in 4R can be translated and the PC α subunit and linker proteins that derive from these transcripts are functional and can be incorporated into a phycobilisome. Thus, the *cpcB* gene is implicated as a possible site of mutation that leads to the 4R phenotype. The DNA sequence analysis of the *cpcBA* from *Synechocystis* sp. strain 6803 WT will be reported elsewhere. Sequence information available for the *cpcBA* region has allowed a comparison between the *cpcB* genes of WT and 4R. The two genes show a single nucleotide difference where 4R *cpcB* has a C insertion at the 73rd nucleotide position (data not shown). The resulting frameshift causes premature termination of translation and would, by prediction, yield a 32-amino-acid peptide of which the first 23 residues correspond to the PC β subunit (CpcB) from WT (Fig. 4). The absence of CpcB in 4R would prohibit the formation of PC monomers and may explain the PC-minus phenotype of 4R on the basis of the simple assumption that unassembled material is degraded.

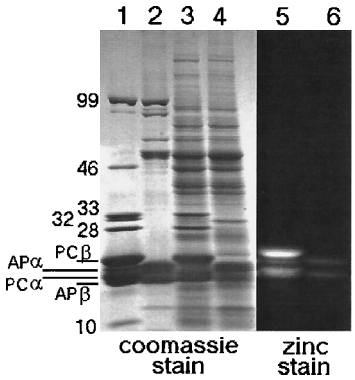

FIG. 2. SDS-PAGE of phycobilisomes and cell extracts. Lanes: 1, phycobilisomes from WT; 2, phycobilisomes from 4R; 3, WT cell extract; 4, 4R cell extract; 5 and 6, same tracks as those in lanes 3 and 4, prior to Coomassie staining, showing zinc-enhanced fluorescence of the bilins. Molecular masses (in kilodaltons) for some phycobilisome proteins are listed to the left the WT sample. The major biliprotein subunits are identified by name. Strain 4R shows the absence of PC subunits in phycobilisomes and in cell extracts (note the lack of fluorescent signals in the zinc stain). Gel images were obtained with a UVP Imagestore 7500 and were composed as figures with Aldus Photostyler software on PC-compatible hardware.

Complementation of the PC-minus phenotype. While the previous results suggest a viable explanation for the PC-minus phenotype in 4R, the origin of this strain as a revertant from a photosynthetic mutant background raises the possibility that mutations outside the *cpc* operon may contribute to the phenotype. Figure 5 shows a restriction map of the 9.6- and 3.8-kbp fragments of WT chromosomal DNA containing the *cpc* operon that were cloned into pBluescriptSK$^-$, creating pPC396 and pPC338, respectively. The 4R strain was transformed with pPC396 and pPC338 by direct application of plasmid DNA to cyanobacterial cells in top agar (13) without antibiotic selection or glucose in the base BG-11 agar. Conversion to a WT phenotype occurred in the immediate radius of the site at which 5 to 10 μg of pPC396 or pPC338 was applied to the top agar. Control areas on the same plates that were treated with 5 to 10 μg of pBluescriptSK$^-$ showed no transformants. While both plasmids produced reversion phenotypes, pPC338 transformants were much less frequent and were harvested from the 4R background with the aid of a dissecting microscope. Multiple transformants were isolated and segregated, and each clone displayed the absorbance, fluorescence energy transfer, and phycobilisome composition of *Synechocystis* sp. strain 6803 WT, indicating the synthesis of a complete PC β subunit and the correction of the *cpcB* lesion in 4R (data not shown). One of the pPC338 transformant clones,

```
WT CpcB    MFDVFTRVVSQADARGEYLSGSQLDALSATVAE...

4R CpcB    MFDVFTRVVSQADARGEYLSGSQLRCFERYRC

α-helices      [-------- X ---------]          [----------- Y -----------]
```

FIG. 4. Consequences of the 4R mutation. The predicted amino acid sequences for CpcB from WT and 4R are presented for the first 33 residues. The X and Y α-helices from the PC structure are lined up with the amino acid sequences. The nucleotide insertion in 4R causes a reading frame shift that introduces a stop codon early in the CpcB primary structure.

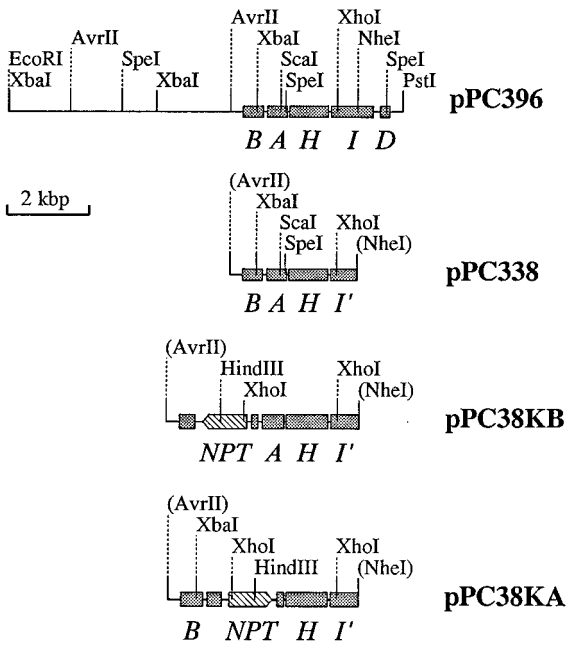

FIG. 5. Maps of plasmid inserts containing the *cpc* operon and interposon mutations. All inserts are cloned in pBluescript SK$^-$. See text for discussion.

R38, was analyzed by Northern hybridization and displayed PC mRNA at levels seen in both WT and 4R strains (Fig. 3, lane 3). Recombination of the WT *cpcB* on pPC338 with the 4R genome would correct the frameshift mutation and produce a PC β subunit that would complement the 4R mutation. Since the CpcA, CpcH, and CpcI proteins in 4R are functional when rescued by heterologous assembly (31), the complementing DNA in pPC338 must reside in the 600-bp region that includes the *cpcB* gene and 200 bp of noncoding DNA upstream of *cpcB*.

Generation of PC-minus phenotypes by interposon mutations. Analysis of the 4R strain shows an absolute requirement of CpcB for stable PC expression. Is there a similar requirement for CpcA? We addressed this question by constructing PC-minus mutants in the WT background using interposon mutagenesis. Plasmid pPC338 was used as the base transformation vector. A neomycin phosphotransferase gene (*npt*) was inserted at the *Xba*I restriction site in *cpcB* and at the *Sca*I restriction site in *cpcA*, creating pPC338KB and pPC338KA, respectively (Fig. 5). *Synechocystis* sp. strain 6803 WT was then transformed with pPC338KB and pPC338KA, and transformants were selected on BG-11 agar supplemented with glucose and kanamycin. Complete segregation of the PC-minus transformants was confirmed by Southern hybridization analysis of chromosomal DNA using *cpc* probes (data not shown). Both interposon mutant strains, W38KB and W38KA, have PC-minus phenotypes that are identical to 4R. Examination of the *cpc* transcript levels suggests that the two mutants are PC minus for different reasons. The *cpcB* mutant W38KB has significantly reduced levels of PC mRNA (Fig. 3, lane 4) that may be attributed to the orientation of the *npt* gene against the direction of *cpc* transcription. Transcription from *npt* may interfere with *cpc* transcription, or part of the *npt* transcript can be antisense relative to the *cpcB* transcript. The W38KA mutant has the *npt* gene inserted in *cpcA* in the same orientation as the *cpc* operon. mRNA from W38KA shows a major PC transcript that is less stable and slightly smaller than the 1.4-kb transcripts in WT and 4R (Fig. 3, lane 5). The *cpc* probe for this Northern hybridization is specific for the DNA region before the *npt* insertion site and indicates the presence of transcripts that initiate from the *cpc* promoter and include *cpcB*. The *npt* insertion in W38KA occurs 160 nucleotides before the end of *cpcA* and introduces translational stop codons in all three reading frames within 60 bp of the *cpcA-npt* junction. Assuming that the major *cpc* transcript in W38KA is translated, the products would consist of an intact CpcB and at least 70% of CpcA. The absence of PC in W38KA implies that the truncated CpcA is not stable and is rapidly degraded, leaving CpcB without an assembly partner and subject to proteolysis.

Immunoblot screening of PC-minus mutants for abandoned subunits. In light of the PC-minus phenotypes in W38KA and 4R, it appears that mutations which truncate either PC subunit may lead to the complete absence of intact partner subunits, possibly through degradation. We reasoned that trace amounts of the abandoned subunits could exist for a short time in these mutants and that more-sensitive methods might detect them in cell extracts. The nature of the abandoned proteins prior to proteolysis, whether they contained chromophore or not, might provide a window on early events in the biliprotein biosynthetic pathway. We used polyclonal antibodies raised against SDS-PAGE-purified CpcA and CpcB from *Synechocystis* sp. strain 6803 in immunoblot analyses of cyanobacterial cell extracts. Strain 4R was transformed with pPC338KA to create a CpcA$^-$ mutant (designated R38KA) for direct comparison with 4R in the immunoblots. apo-PC subunits (synthesized in vitro) were used to indicate the positions in SDS-PAGE of CpcA and CpcB that lacked chromophores. The detection limit of anti-CpcA in immunoblots was tested under our standard conditions with a dilution series of purified PC, demonstrating a clear detection of 1 ng of CpcA (data not shown). Anti-CpcB was not assayed for a lower detection limit; however, comparative immunoblots have shown it to be less sensitive than that for anti-CpcA.

If abandoned subunits are detectable by immunoblot, extracts of 4R should contain CpcA while R38KA and W38KA are predicted to be CpcA negative because of interposon mutations. The W38KA extract may display CpcB, but 4R and R38KA should both be CpcB negative because of the reading frame shift in *cpcB*. Strain W38KB should be negative for both CpcA and CpcB on the basis of the level of *cpc* transcripts in this mutant (Fig. 3). Figure 6A shows an anti-CpcA immunoblot against cell extracts from 4R, R38KA, W38KA, and W38KB. All four extracts contain two immunoreactive proteins that migrated close to the major signal in the purified PC control lane, and none of the cell extracts indicated the presence of apo-CpcA. The zinc-enhanced fluorescence from the same gel shows that the major fluorescence signals are due to AP subunits and that anti-CpcA exceeds fluorescence in detection sensitivity for SDS-PAGE (note the weak fluorescence in the PC control lane). These results suggested that the polyclonal anti-CpcA was detecting other proteins that comigrated with CpcA in SDS-PAGE. This is a distinct possibility, since the CpcA antigen was isolated by electroelution of gel slices from high-resolution SDS-PAGE of *Synechocystis* sp. strain 6803 phycobilisomes. We employed SDS-PAGE in the presence of 8 M urea to alter protein mobility during electrophoresis (6) in an effort to unmask any trace amounts of CpcA in 4R (Fig. 6B). The major signals detected by anti-CpcA in all four extracts did not comigrate with CpcA in the PC control lane, and there was no detectable protein in 4R that was missing in the other three samples. Anti-CpcB was also tested against the

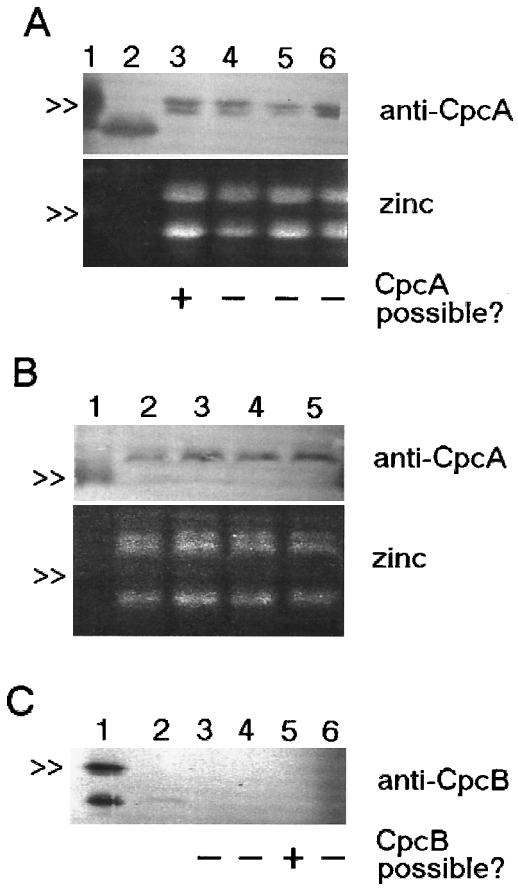

FIG. 6. Immunoblot analysis of PC contents in WT and mutant strains. (A) Standard SDS-PAGE of cell extracts; the upper panel is an immunoblot with anti-CpcA, and the lower panel is a zinc stain of the same tracks prior to transfer to nitrocellulose. Lanes: 1, isolated PC; 2, in vitro transcription-translation extract with pPC02 as a template; 3, 4R; 4, R38KA; 5, W38KA; 6, W38KB. Only lane 3 is expected to show CpcA if it is there. Double carets mark the positions of CpcA. (B) SDS-PAGE in 8 M urea of cell extracts; upper and lower panels are as in panel A. Lanes: 1, isolated PC; 2, 4R; 3, R38KA; 4, W38KA; 5, W38KB. Double carets mark the positions of CpcA. (C) Standard SDS-PAGE of cell extracts and immunoblot with anti-CpcB. Lanes are identical to those in panel A, but only lane 5 is expected to show CpcB if it is there. Double carets mark the position of CpcB. Gel images were obtained with a UVP Imagestore 7500 and were composed as figures with Aldus Photostyler software on PC-compatible hardware.

four cell extracts, purified PC, and apo-CpcB (Fig. 6C) and showed no CpcB signals in any of the extracts.

The immunoblot results establish that these cell extracts do not contain abandoned PC subunits. If CpcA is present in 4R prior to degradation, the yield recoverable by our methods must be less than 1 μg of protein per liter of cell culture on the basis of the detection capability of anti-CpcA. It is possible that this simple extraction procedure does not preserve the proteins of interest. We have used multiple protease inhibitors in addition to phenylmethylsulfonyl fluoride in the cell extraction procedure, including EDTA, benzamidine, ε-amino caproic acid, and leupeptin. We have also achieved a more-rapid, less-efficient extraction by grinding cells in liquid nitrogen with a mortar and pestle. No combination of these modified protocols produced data that supported the presence of CpcA or CpcB in any of the cell extracts.

In summary, strains 4R and W38KA have mutations that truncate the CpcB and CpcA proteins, respectively, and both mutants have a complete PC-minus phenotype in spite of PC mRNA levels that are comparable to that of the WT strain. Inability to detect trace amounts of CpcA or CpcB as the stranded partners in each mutant suggests that nascent biliprotein subunits are rapidly and immediately degraded in the absence of their assembly partner or that unassembled subunits may initiate a process that blocks translation from the *cpc* transcripts.

DISCUSSION

Origin of the complete PC-minus phenotype in 4R. An explanation for the complete absence of CpcA in 4R must accommodate the high level of *cpc* transcripts in this strain. The rescue of 4R CpcA by heterologous assembly (31) rules out polarity effects in which the synthesis of CpcA would require translation through *cpcB*. The simplest explanation for the 4R phenotype is based on a proteolytic activity that degrades abandoned subunits in a rapid and efficient manner. This activity could be constitutive, or the production of unassembled biliprotein subunits may be similar to the synthesis of abnormal proteins, which is known to induce protease activities as part of a heat shock-like response in *E. coli* (21, 26). The degradation of proteins that lack assembly partners should be reciprocal with respect to α and β subunits and was demonstrated in comparisons of the 4R and W38KA strains. Degradation of unassembled subunits should affect other biliprotein classes as well, and this was observed for a nonsense mutation that terminates ApcA in the middle of the F-helix and causes a complete AP-minus phenotype in the UV6p strain of *Synechocystis* sp. strain 6803 (40).

Subunit interactions and biliprotein stability. Formation of the monomer by the PC β and α subunits is accompanied by the burial of 1,040 $Å^2$ (1 Å = 0.1 nm) of surface area and is mediated predominantly by conserved hydrophobic residues (5, 38). The monomer is quite stable and requires high concentrations of urea (19) or 63 mM formic acid (30) to separate the subunits. Trimers and hexamers exist in an equilibrium with the monomers that can be affected by moderate changes in protein concentration, salt concentration, and pH (18). The complete absence of CpcA in 4R is in strong contrast with the PC content of another PC assembly mutant, strain UV16 of *Synechocystis* sp. strain 6701 (2–4). A mutation in the CpcA of UV16 blocks the formation of PC hexamers, yet this strain contains soluble trimers and monomers at 30% of the wild-type PC level. This difference between 4R and UV16 suggests the existence of a rapid and efficient salvage mechanism that primarily recognizes unassembled subunits over the higher-order biliprotein complexes. Since the α and β subunits of PC do not show significant structural changes upon monomer formation (30), the degradation process must be initiated by exposure of hydrophobic residues in the subunit interface domain that are buried upon monomer formation.

If subunit interactions can protect the biliproteins from degradation, why does the W38KA strain have a PC-minus phenotype? CpcA in W38KA would be missing 28% of the C terminus because of the interposon mutation; however, inspection of the structure (12) shows that this part of the protein has no direct involvement in the subunit interface and that all contact residues for a monomer would be intact in the truncated CpcA. The instability of CpcA in W38KA must derive exclusively from the absence of the C terminus, which could expose new sites for proteolysis, or it might affect protein folding if the biliproteins utilize a folding pathway that has been proposed for the structurally related myoglobin (8, 24, 25). Either case would yield a stranded CpcB protein that is also subject to rapid degradation. The importance of the C

terminus for subunit stability can also be seen in the UV6p mutant (40), in which truncation of ApcA in the middle of the F-helix causes complete loss of both ApcA and ApcB.

Conclusion. Mutations that disrupt the structure of one biliprotein subunit can result in the phenotypic absence of both subunits. The major difference between a stranded subunit and a monomer-bound subunit is the exposure of the subunit-binding domain to the environment, and stable expression of a biliprotein requires protection of this domain by formation of the monomer. Since degradation of stranded subunits appears to be quite rapid, the early events of biliprotein biosynthesis, which include folding, covalent modifications (14, 15, 41), and subunit interactions, must occur with a speed and precision that prevent unwanted proteolysis of functional proteins.

ACKNOWLEDGMENTS

We thank Susan Hettenbach for excellent technical assistance. Synthetic oligonucleotides were obtained from the Oklahoma Molecular Biology Resource Facility, under the direction of Ken Jackson.

This work was supported by grants from the Army Research Office (29537-LS), the Department of Defense (32096-LS-AAS), and the Oklahoma Center for the Advancement of Science and Technology (HN0-004 no. 4473).

REFERENCES

1. **Anderson, L. K., and F. A. Eiserling.** 1986. Asymmetrical core structure in phycobilisomes of the cyanobacterium *Synechocystis* sp. 6701. J. Mol. Biol. **191:**441–451.
2. **Anderson, L. K., and A. R. Grossman.** 1990. Genes for phycocyanin subunits in *Synechocystis* sp. strain 6701 and assembly mutant UV16. J. Bacteriol. **172:**1289–1296.
3. **Anderson, L. K., M. C. Rayner, and F. A. Eiserling.** 1984. Ultra-violet mutagenesis of *Synechocystis* sp. 6701: mutations in chromatic adaptation and phycobilisome assembly. Arch. Microbiol. **138:**237–243.
4. **Anderson, L. K., M. C. Rayner, and F. A. Eiserling.** 1987. Mutations that affect structure and assembly of light-harvesting proteins in the cyanobacterium *Synechocystis* sp. strain 6701. J. Bacteriol. **169:**102–109.
5. **Apt, K. E., J. L. Collier, and A. R. Grossman.** 1995. Evolution of the phycobiliproteins. J. Mol. Biol. **248:**79–96.
6. **Bryant, D. A.** 1981. The photoregulated expression of multiple phycocyanin species. Eur. J. Biochem. **119:**425–429.
7. **Bryant, D. A.** 1991. Cyanobacterial phycobilisomes: progress towards a complete structural and functional analysis via molecular genetics, p. 257–300. *In* L. Bogorad and I. K. Vasil (ed.), The photosynthetic apparatus: molecular biology and operation. Academic Press, Inc., San Diego, Calif.
8. **Chelvanayagam, G., Z. Reich, R. Bringas, and P. Argos.** 1992. Prediction of protein folding pathways. J. Mol. Biol. **227:**901–916.
9. **Chisholm, D.** 1990. Microfuge miniprep for *Synechocystis* PCC 6803 chromosomal DNA, p. 7. *In* J. Elhai (ed.), Cyanonews, vol. 6. Florida International University, Miami.
10. **de Lorimier, R., G. Guglielmi, D. A. Bryant, and S. E. Stevens.** 1990. Structure and mutation of the gene encoding the M_r 33,000 phycocyanin-associated linker polypeptide. Arch. Microbiol. **153:**541–549.
11. **Duerring, M., R. Huber, W. Bode, R. Ruembeli, and H. Zuber.** 1990. Refined three-dimensional structure of phycoerythrocyanin from the cyanobacterium *Mastigocladus laminosus*. J. Mol. Biol. **211:**633–644.
12. **Duerring, M., G. B. Schmidt, and R. Huber.** 1991. Isolation, crystallization, crystal structure analysis and refinement of constitutive C-phycocyanin from the chromatically adapting cyanobacterium *Fremyella diplosiphon*. J. Mol. Biol. **217:**577–590.
13. **Dzelkalns, V. A., and L. Bogorad.** 1988. Molecular analysis of a mutant defective in photosynthetic oxygen evolution and isolation of a complementing clone by a novel screening procedure. EMBO J. **7:**333–338.
14. **Fairchild, C. D., and A. Glazer.** 1994. Oligomeric structure, enzyme kinetics, and substrate specificity of the phycocyanin α subunit phycocyanobilin lyase. J. Biol. Chem. **269:**8686–8694.
15. **Fairchild, C. D., J. Zhao, J. Zhou, S. E. Colson, D. A. Bryant, and A. N. Glazer.** 1992. Phycocyanin α-subunit phycocyanobilin lyase. Proc. Natl. Acad. Sci. USA **89:**7017–7021.
16. **Ficner, R., K. Lobeck, G. Schmidt, and R. Huber.** 1992. Crystal structure and refinement of B-phycoerythrin from *Porphyridium sordidum*. J. Mol. Biol. **228:**935–950.
17. **Gingrich, J. C., L. K. Blaha, and A. N. Glazer.** 1982. Rod substructure in cyanobacterial phycobilisomes: analysis of *Synechocystis* sp. 6701 mutants low in phycoerythrin. J. Cell Biol. **92:**261–268.
18. **Glazer, A. N.** 1976. Phycocyanins: structure and function. Photochem. Photobiol. Rev. **1:**71–115.
19. **Glazer, A. N., and S. Fang.** 1973. Formation of hybrid proteins from the α and β subunits of phycocyanins of unicellular and filamentous blue-green algae. J. Biol. Chem. **248:**663–671.
20. **Glazer, A. N., D. J. Lundell, G. Yamanaka, and R. C. Williams.** 1983. The structure of a "simple" phycobilisome. Ann. Inst. Pasteur Microbiol. **134B:** 159–180.
21. **Goff, S. A., and A. L. Goldberg.** 1985. Production of abnormal proteins in *E. coli* stimulates transcription of *lon* and other heat shock genes. Cell **41:**587–595.
22. **Harlow, E., and D. Lane.** 1988. Antibodies: a laboratory manual. Cold Spring Harbor Laboratory Press, Cold Spring Harbor, N.Y.
23. **Hovanessian, A. G., J. Galabru, Y. Riviere, and L. Montagnier.** 1988. PolyA · polyU as an adjuvant. Immunol. Today **9:**161–162.
24. **Hughson, F., P. E. Wright, and R. L. Baldwin.** 1990. Structural characterization of a partly folded apomyoglobin intermediate. Science **249:**1544–1548.
25. **Jennings, P. A., and P. E. Wright.** 1993. Formation of a molten globule intermediate early in the kinetic folding pathway of apomyoglobin. Science **262:**892–896.
26. **Kanemori, M., H. Mori, and T. Yura.** 1994. Induction of heat shock proteins by abnormal proteins results from stabilization and not increased synthesis of σ^{32} in *Escherichia coli*. J. Bacteriol. **176:**5648–5653.
27. **Laemmli, U. K.** 1970. Cleavage of structural proteins during the assembly of the head of bacteriophage T4. Nature (London) **227:**680–685.
28. **Lundell, D. J., and A. N. Glazer.** 1983. Molecular architecture of light harvesting antenna. Structure of the 18S core-rod subassembly of *Synechococcus* 6301 phycobilisomes. J. Biol. Chem. **258:**8708–8713.
29. **Lundell, D. J., R. C. Williams, and A. N. Glazer.** 1981. Molecular architecture of a light-harvesting antenna. In vitro assembly of the rod substructures of *Synechococcus* 6301 phycobilisomes. J. Biol. Chem. **256:**3580–3592.
30. **Mimuro, M., P. Fuglistaller, R. Rumbeli, and H. Zuber.** 1986. Functional assignment of chromophores and energy transfer in C phycocyanin isolated from the thermophilic cyanobacterium *Mastigocladus laminosus*. Biochim. Biophys. Acta **848:**155–166.
31. **Plank, T., and L. K. Anderson.** 1995. Heterologous assembly and rescue of stranded phycocyanin subunits by expression of a foreign *cpcBA* operon in *Synechocystis* sp. strain 6803. J. Bacteriol. **177:**6804–6809.
32. **Raps, S.** 1990. Differentiation between phycobiliproteins and colorless linker polypeptides by fluorescence in the presence of $ZnSO_4$. Plant Physiol. **92:** 358–362.
33. **Reddy, K. J., R. Webb, and L. A. Sherman.** 1990. Bacterial RNA isolation with one hour centrifugation in a tabletop centrifuge. BioTechniques **8:**250–251.
34. **Rippka, R., J. Deruelles, J. B. Waterbury, M. Herdman, and R. Y. Stanier.** 1979. Generic assignments, strain histories and properties of pure cultures of cyanobacteria. J. Gen. Microbiol. **111:**1–62.
35. **Saiki, R.** 1990. Amplification of genomic DNA, p. 13–20. *In* M. A. Innis, D. H. Gelfand, J. J. Sninsky, and T. J. White (ed.), PCR protocols. Academic Press, Inc., San Diego, Calif.
36. **Sambrook, J., E. F. Fritsch, and T. Maniatis.** 1989. Molecular cloning: a laboratory manual. Cold Spring Harbor Laboratory Press, Cold Spring Harbor, N.Y.
37. **Schirmer, T., W. Bode, and R. Huber.** 1987. Refined three-dimensional structures of two cyanobacterial phycocyanins. A common principle of phycobilin-protein interaction. J. Mol. Biol. **196:**677–695.
38. **Schirmer, T., W. Bode, R. Huber, W. Sidler, and H. Zuber.** 1985. X-ray crystallographic structure of the light-harvesting biliprotein C-phycocyanin from the thermophilic cyanobacterium *Mastigocladus laminosus* and its resemblance to globin structure. J. Mol. Biol. **184:**257–277.
39. **Schirmer, T., R. Huber, M. Schneider, W. Bode, M. Miller, and M. Hackert.** 1986. Crystal structure analysis and refinement at 2.5 angstroms of hexameric C-phycocyanin from the cyanobacterium *Agmenellum quadruplicatum*. J. Mol. Biol. **188:**651–676.
40. **Su, X., P. G. Fraenkel, and L. Bogorad.** 1992. Excitation energy transfer from phycocyanin to chlorophyll in an *apcA*-defective mutant of *Synechocystis* sp. 6803. J. Biol. Chem. **267:**22944–22950.
41. **Thomas, B. A., L. P. McMahon, and A. V. Klotz.** 1995. N^5-methylasparagine and energy-transfer efficiency in C-phycocyanin. Biochemistry **34:**3758–3770.
42. **Walker, B., and H. Bayley.** 1994. A pore-forming protein with a protease-activated trigger. Protein Eng. **7:**91–97.
43. **Williams, J. G. K.** 1988. Transformation in the unicellular cyanobacterium *Synechocystis* sp. 6803. Methods Enzymol. **167:**766–778.